Cisplatin-DNA Adducts by Vibrational Circular Dichroism Spectroscopy: Structure and Isomerization of d(CCTG*G*TCC)·d(GGACCAGG) Intrastrand Cross-Linked by Cisplatin

Dimiter Tsankov,[†,‡] Berndt Kalisch,[#] Hans van de Sande,[#] and Hal Wieser*[,†]

Department of Chemistry, Faculty of Science, and Department of Biochemistry and Molecular Biology, Faculty of Medicine, University of Calgary, Calgary, AB, T2N 1N4, Canada

Received: January 30, 2003; In Final Form: March 20, 2003

The intrastrand cisplatin adduct of the duplex d(CCTG*G*TCC)·d(GGACCAGG), where the asterisks denote the 1,2-intrastrand crosslink, was synthesized and studied in solution in D_2O by vibrational circular dichroism (VCD) and infrared absorption spectroscopy. Comparison of the spectra of the platinated and unmodified complexes confirmed that the entire structure is considerably distorted, as a result of the platinum coordination to the octamer duplex. The major changes in the VCD spectra were detected in the fourth base step, where the cisplatin cross-links the adjacent guanine bases G4 and G5. Platinum coordination shifts the G4−C13 and G5−C12 base pairs apart, with a concomitant disruption of the stacking between the neighboring bases T3−G4 and G5−T6. The resultant new VCD couplets were assigned to stacking interactions between A11 and A14, which implies a substantially distorted structure. Slow isomerization is indicated by diagnostic changes in VCD, converting the *intra*strand adduct to other adducts. The corresponding absorption spectra remain essentially unchanged. This DNA octamer was previously studied by NMR in great detail when the isomerization was first detected after one day. Our measurements show that the conversion began soon after both strands were annealed and the first signs were detected in 2 h. This investigation again demonstrated convincingly that VCD is very sensitive to DNA structure modified by complex formation with cisplatin and may become more widely applicable for other similar applications.

Introduction

The compound *cis*-diamminedichloroplatinum(II) (*cis*-DDP) is a widely used anticancer drug[1,2] that binds to DNA in the cell, thereby inhibiting replication.[3−5] When *cis*-DDP reacts with DNA, various stable bifunctional adducts are formed. The major species arises from 1,2-*intra*strand crosslinks of *cis*-DDP with adjacent guanine (G) or adenine (A) bases, which, together, account for 90% of the bound platinum. Other adducts involve *cis*-DDP *intra*strand crosslinks to 1,3-d(GXG), as well as various *inter*strand crosslinks.[6−8] The *intra*strand adducts with guanine and adenine were thought to be responsible for the cytotoxic activity of cisplatin, since they were found in cancer patients who were successfully treated with this drug.[9] This result was questioned,[10] because the relative distribution of these adducts is quite different for carboplatin [(*cis*-diammine-1,1-cyclobutyldicarboxylato)platinum(II)].[11,12] This second-generation cisplatin drug yields practically the same DNA adducts but with a different distribution, where 1,3-d(GXG) is the prominent crosslink.[10]

Solution and crystal studies of platinated duplex DNA confirmed that platinum binds to N7 of two neighboring guanines, and that the sugar ring has endo-conformation.[13−18] X-ray crystallographic data provided a set of interatomic distances and dihedral angles for the structure. As a result of platination, the purine bases are completely destacked, reaching dihedral angles of 75°−90° instead of the usual ±10° in unplatinated B-DNA. This unstacking leads to pronounced bending toward the major groove in DNA at the site of platination, to local unwinding of the helix, and to a concomitant widening and flattening of the minor groove.

Such structural distortions should be amenable, in principle, to monitoring by vibrational circular dichroism (VCD) spectroscopy, which could provide another view of DNA interaction with cisplatin. The enhanced stereochemical sensitivity of VCD shows its advantage, particularly in this application, compared to electronic circular dichroism and conventional absorption spectroscopy. Well-resolved features in the spectra, known as *couplets* (consisting of close-lying positive and negative components), arise from "coupled" vibrations of identical oscillators, as explained by the exciton model.[19−22] The couplets are said to be either *positive* or *negative* when the component at a *lower* wavenumber is either *positive* or *negative*, respectively. Although the bases and deoxyribose−phosphate backbone themselves are inherently achiral, the dissymmetric helical structure of DNA gives rise to these distinctive features, which then reveal specific details about base sequences and stacking interactions.

Two regions between 1800 and 800 cm^{-1} are of particular interest, namely those of various nitrogen base modes (1730−1460 cm^{-1}) and those of sugar−phosphate backbone vibrations (1170−800 cm^{-1}). The former originate from carbonyl stretching and in-plane deformation modes of the purines and pyrimidines. The second region contains the symmetric PO_2^- stretching vibrations, as well as C−O stretching and various sugar deformation modes. VCD signals arising from PO_2^- stretching can monitor backbone structure, whereas sugar puckering vibrations at lower wavenumbers can help identify deoxyribose conformations. The region below 800 cm^{-1} is

* Author to whom correspondence should be addressed. E-mail: hwieser@ucalgary.ca.

[†] Department of Chemistry, Faculty of Science.

[‡] Permanent address: Institute of Organic Chemistry, Bulgarian Academy of Sciences, 1113 Sofia, Bulgaria.

[#] Department of Biochemistry and Molecular Biology, Faculty of Medicine.

10.1021/jp034246c CCC: $25.00
Published on Web 06/06/2003

currently not routinely accessible for VCD measurements, because of restrictions imposed by the VCD optics that are commonly used. A possible extension of the measurements down to 600 cm^{-1} could be very beneficial, given the important role that sugar-backbone vibrations play in conformation-related functions of DNA.

With the work described here, we intended to achieve the following two objectives. On the basis of our previous experiences, we wanted to extend our understanding of structural changes of DNA when coordinated with metal ions by applying VCD to *cis*-DDP-oligonucleotide adducts. More importantly, for further investigations of cisplatin complexes by VCD, it will be essential to correlate VCD features with structures determined by other means, specifically NMR[13,14] and X-ray crystallography,[17,18] thereby establishing whether VCD is capable of providing information complementary to NMR and X-ray and revealing new and/or different structural aspects. Pioneering studies, particularly from the laboratories of T. Keiderling and M. Diem, have clearly demonstrated the capabilities of VCD for investigating DNA structures.[23,24] In our laboratory, we applied this method to selected oligonucleotides, to monitor structural and conformational changes in DNA and oligonucleotides when complexed with intercalating drugs[25−27] and metal ions.[28−33] This paper presents the first observation of a platinated DNA adduct by VCD spectroscopy, for which we examined the octamer duplex d(CCTG*G*TCC)·d(GGACCAGG) in aqueous solution. The asterisks in this notation denote the *cis*-DDP binding site. As an additional outcome, the results confirmed that this adduct appeared metastable, even at 2 °C. The VCD spectra showed evidence, not apparent in absorption, that slow isomerization started after ∼2 h, converting the adduct to other forms.[13]

Materials and Methods

Single-stranded d(CCTGGTCC) (GG) and its complementary octamer d(GGACCAGG) (CC) were synthesized in the University of Calgary Core DNA Services facility, using standard solid-phase phosphoamidite methods, followed by size exclusion chromatography (Sephadex model G25) for purification. *cis*-Diamminedichloroplatinum(II) was purchased from Sigma. D_2O (99.5% isotopic purity), obtained from Aldrich, was used as the solvent for VCD and absorption spectroscopy.

The activated diaquo form of cisplatin was prepared as described previously[14] by allowing 1.97 equiv of $AgNO_3$ to react with *cis*-$[Pt(NH_3)_2Cl_2]$ in water at room temperature overnight. The next day, the reaction mixture was centrifuged for 10 min, the aqueous layer was removed by pipetting, and then the mixture was centrifuged again to get rid of possible AgCl remnants. The supernatant so obtained was allowed to react with the GG strand in an aqueous solution buffered to pH 6.0 with 10 mM sodium phosphate. The GG strand and *cis*-$[Pt(NH_3)_2(H_2O)_2]$ were added in a *cis*-Pt/strand molar ratio of 1.3:1 and incubated at 37 °C in the dark for 24 h and then kept for two days at room temperature.

The extent of the modification was controlled by taking aliquots and end-labeling with T_4 polynucleotide kinase and ^{32}P-ATP.[15] The labeled samples were run on 15% denaturing polyacrylamide gels. The mobility of the modified deoxyoligonucleotide was just above the unmodified control. These gel electrophoresis experiments showed that the addition of *cis*-Pt was greater than 95%. The reaction products were separated by low-pressure anionic exchange chromatography[16] on a DEAE model A-25 column (1.2 cm × 20 cm). A 150 mL (10 mM) × 150 mL (0.8 M) NaCl gradient was used. The modified deoxyoligonucleotide eluted before the unmodified octamer and was the primary peak. It was extensively desalted by exclusion gel filtration (Sephadex model G-25), eluted in double distilled water, and then lyophilized to dryness.

Purified platinated GG and unmodified CC strands, in a 1:1 molar ratio, were dissolved separately in 99.5% D_2O and lyophilized to dryness. Complete deuterium exchange was achieved after lyophilizing three times and redissolving in D_2O. Finally, both strands were annealed by slow cooling from 70 °C in a D_2O solution that had been buffered to pD 6.25 with 40 mM sodium cacodylate and 60 mM NaCl. The final duplex concentration was 15 mM. The DNA melting curve obtained for the platinated duplex indicated a melting temperature of 18 °C.

The absorption and VCD measurements were performed with the instrument described elsewhere.[34] All spectra were recorded in the 1800−800 cm^{-1} range with a resolution of 4 cm^{-1}. The region between ∼1300 and 1150 cm^{-1}, which contains the asymmetric PO_2^- stretching vibrations, is excluded from the spectra displayed in the figures shown later in this work, because of the strong absorption of D_2O. The samples were held in a custom infrared cell consisting of two BaF_2 windows separated by a 45 μm Teflon spacer. A special cooling chamber purged with dry nitrogen maintained the temperature at 2.0 ± 0.1 °C, using a circulating water thermostat (NESLAB Instruments, Inc.) controlled by a copper-constantan thermocouple (OMEGA Technology Company, Inc.). The infrared beam was modulated by a ZnSe photoelastic modulator (Hinds International) for the VCD measurements. For the unplatinated octamer duplex, 7500 sample scans (designated "ac", total collection time of ∼2 h, 55 min) were accumulated to achieve good signal-to-noise ratio and flat baselines. These scans were ratioed against 500 unmodulated scans (designated "dc", total collection time of ∼10 min). In view of the expected isomerization,[10] only 2500 ac scans were collected in succession for the platinated duplex (∼1 h scan time for each) and ratioed against the average of two 50 dc scans (∼2 min for each; one taken before and the other after the accumulation of the ac scans). The VCD spectra of the samples were corrected for baseline distortions and polarization artifacts by subtracting the VCD spectra of the solvent taken under the same experimental conditions.

The VCD and absorption spectra are displayed in Figure 1 for the duplex alone and in Figure 2 for the platinated duplex. The stacking sequence of the nucleic acids (Chart 1) will be helpful for the discussion of the results given later in this work. The wavenumber positions of the absorption bands and the VCD signals, including the assignments, are summarized in Table 1.

When inspecting the figures, one quickly realizes that interpreting the spectra and assigning the bands to particular vibrational modes is likely to be difficult, the apparent higher resolution and very distinct changes between the unplatinated and platinated duplex notwithstanding. The assignments we propose here are based on multiple experiences with oligonucleotide and DNA systems,[25−33,35−37] for which various positions are remarkably reproducible. By the same token, both the base and phosphate modes are likely to couple, unmistakably yielding the typical VCD signatures. We cannot definitively settle the question of whether several of the smaller features may be noise in the spectra, but we did refrain from venturing into regions of the VCD spectra where noise becomes distinctly noticeable and the peak positions are not reproducible. Although it is customary for VCD to record noise estimates, this luxury was not an option, because the octamer−cisplatin complex changes with time (see below).

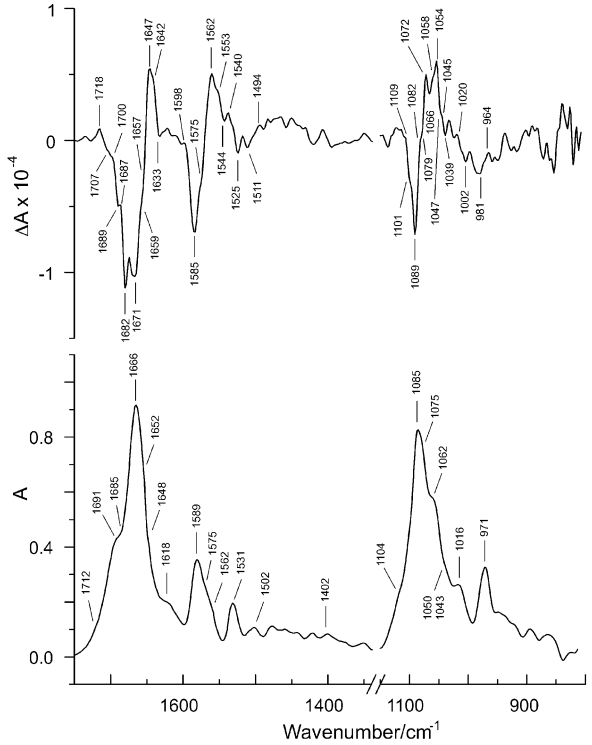

Figure 1. VCD (top) and absorption (bottom) spectra of the d(CCTGGTCC)·d(GGACCAGG) in D_2O. Conditions were as follows: 1800−800 cm^{-1}, 4 cm^{-1} resolution; 2.0 ± 0.1°C; BaF_2 windows with a path length of 45 μm; 7500 ac scans for samples (2 h, 55 min) ratioed against 500 dc scans for the solvent (30 min).

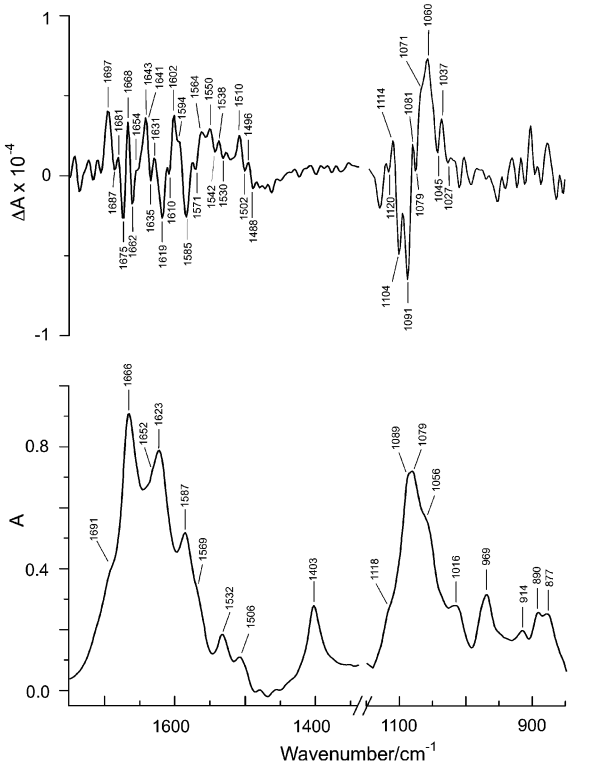

Figure 2. VCD (top) and absorption (bottom) spectra of the d(CCTGGTCC)·d(GGACCAGG)−cisplatin complex in D_2O. Conditions were as follows: 1800−800 cm^{-1}, 4 cm^{-1} resolution; 2.0 ± 0.1°C; BaF_2 windows with a path length of 45 μm; 2500 ac scans for samples (∼1 h) ratioed against 50 dc scans for solvent (∼2 min).

Results

d(CCTGGTCC)·d(GGACCAGG) (I). The VCD and absorption spectra of the unmodified duplex (Figure 1, Table 1) are typical of the B-family of DNA.[27,38] The VCD couplets at 1718(+)/1707(−) and 1700(+)/1689(−) cm^{-1}, corresponding to the visible shoulders in absorption near 1712 and 1691 cm^{-1}, respectively, are typical for the carbonyl stretching of C(2) of thymine in different stacking combinations in the double helix.[31] The next negative couplet, at 1687(+)/1682(−) cm^{-1}, together with the 1685 cm^{-1} shoulder in absorption, arise from carbonyl stretching of guanine in one stacking environment.[27,35] The main VCD feature with clear negative and positive peaks at 1671 and 1647 cm^{-1}, respectively, consists of two consecutive couplets at 1671(−)/∼1659(+) and ∼1657(−)/1647(+) cm^{-1}. The first of these, which corresponds to the strongest absorption peak at 1666 cm^{-1}, is assigned to the carbonyl mode of guanine in a stacking environment different from the previous one.[27,35,36] The corresponding absorption for the second of these two couplets is the shoulder at 1652 cm^{-1}, which is ascribed to the C═O stretching of cytosine.[27,35,36,39] The VCD feature at 1642(+)/1633(−) cm^{-1}, with its corresponding shoulder in absorption at 1648 cm^{-1}, arises from the C4═O stretch of thymine.[27,39] The absorption peak at 1618 cm^{-1}, which lacks a visible VCD counterpart, is due to an in-plane ring mode of adenine.[35,37]

The next cluster in absorption also yields a rich set of VCD features, although the multiple features are not necessarily easily resolved. The VCD couplet at ∼1598(+)/1585(−) cm^{-1} corresponds logically to the absorption at 1589 cm^{-1}, and the next positive couplet, at ∼1575(−)/1562(+) cm^{-1}, corresponds to the absorption at 1575 cm^{-1}. High-level ab initio calculations for the GC octamer duplex[36] suggest that both can be assigned to C−N(D_2) stretching of guanine in two different stacking environments. The same calculations enable us to assign the clearly distinguishable couplet at 1553(+)/1544(−) cm^{-1} to C═N stretching of guanine. There is no clearly corresponding absorption band, although the weak shoulder at ∼1562 cm^{-1} must be somehow involved. More easily assigned is the 1540(+)/1525(−) cm^{-1} couplet, which is centered on the 1531 cm^{-1} absorption. It was ascribed to a C═N vibration of guanine.[39] The weak absorption at 1502 cm^{-1} is observed consistently when cytosine is present. Although it can usually be identified by a persistent negative couplet at 1507(+)/1497(−) cm^{-1},[27] and has been identified as the C═N stretching of cytosine,[36] it lacks a clearly visible VCD counterpart here, except perhaps for the weak negative positive couplet at 1511(−)/1494(+) cm^{-1}. The weak absorption at 1402 cm^{-1} originates from a vibration to which the C−N glycosidic bond contributes to a considerable extent.[39]

CHART 1

C1 – C2 – T3 – G4 – G5 – T6 – C7 – C8

G16 – G15 – A14 – C13 – C12 – A11 – G10 – G9

The region between 1140 and 800 cm^{-1} also displays distinctive VCD couplets, the most prominent being the symmetric PO_2^- stretching mode.[27,40] The negatively biased VCD feature at 1109(+)/1101(−) cm^{-1} corresponds to an apparent shoulder in absorption at 1104 cm^{-1}. It has not been identified previously but is seen persistently in other duplexes and likely is due to a C−O stretch of the sugar. The main VCD feature at 1089(−)/1072(+) cm^{-1} consists of two consecutive couplets. One occurs at 1089(−)/∼1082(+) cm^{-1}, and the other at ∼1079(−)/1072(+) cm^{-1}, corresponding to two overlapping absorptions with apparent maxima at 1085 and 1075 cm^{-1}, respectively. In many other B-form duplexes, these overlapped

TABLE 1: Absorption and VCD Data of d(CCTGGTCC)·d(GGACCAGG) Free and Complexed with Cisplatin

	octamer free (**I**) (Figure 1)		octamer−Pt complex (**II**) (Figure 2)	
assignment[a]	absorption	VCD (cm^{-1})	absorption	VCD (cm^{-1})
C2=O stretch of thymine	1712	1718(+)/1707(−)		
	1691	1700(+)/1689(−)	1691	1697(+)/1687(−)
C6=O stretch of guanine	1685	1687(+)/1682(−)	1666	1681(+)/1675(−)
	1666	1671(−)/∼1659(+)		1668(+)/1662(−)
C=O stretch of cytosine	1652	∼1657(−)/1647(+)	1652	1654(−)1643(+)
C4=O stretch of thymine	1648	1642(+)/1633(−)		1641(+)/1635(−)
ring in-plane mode of adenine	1618		1623	1631(+)/1619(−)
				1610(−)/1602(+)
C−N(D_2) stretch of guanine	1589	1598(+)/1585(−)	1587	1594(+)/1585(−)
	1575	1575(−)/1562(+)	1569	1571(−)/1564(+)
C=N stretch of guanine	1562	1553(+)/1544(−)		1550(+)/1542(−)
ring in-plane mode of cytosine	1531	1540(+)/1525(−)	1532	1538(+)/1530(−)
C=N stretch of cytosine	1502	1511(−)/1494(+)	1506	1510(+)/1502(−)
				1496(+)/1488(−)[b]
			1403	
sym PO_2^- plus C−O stretch			1118	1120(−)[b]
	1104	1109(+)/1101(−)	1110	1114(+)/1104(−)
sym PO_2^- stretch	1085	1089(−)/1082(+)	1089	1091(−)/1081(+)
	1075	1079(−)/1072(+)	1079	1079(−)/1071(+)
phosphodiester backbone	1062[b]	1066(−)/1058(+)[b]		
coupled to sugar modes	1050[b]	1054(+)/1047(−)[b]	1056	1060(+)/1045(−)
	1043[b]	1045(+)/1039(−)[b]		1037(+)/1027(−)
	1016		1016	
	971	981(−)/964(+)[b]	969	
sugar modes			914	
	890		890	
			877	

[a] From refs 31, 36, 39, 40, and 41. [b] Assignments/designations uncertain.

VCD and absorption bands appear as one single feature.[27,35] In the unplatinated duplex (**I**), the second of the two bands may be assigned to a sugar vibration.[41] The shoulder in absorption at 1062 cm^{-1} is undoubtedly a sugar mode, probably corresponding to a weak VCD counterpart at 1066(−)/1058(+) cm^{-1}. Other sugar modes are hidden under a broad shoulder at ∼1050 cm^{-1}. Two of these modes give rise to the apparent couplets at 1054(+)/∼1047(−) and ∼1045(+)/1039(−) cm^{-1}. Associated VCD features for the noticeable absorption at 1016 cm^{-1} are difficult to discern definitively, because of noise that is due to the low throughput of light in this region. The prominent absorption at 971 cm^{-1} was assigned as a stretching vibration of deoxyribose involving C(5)−O(5)/C(4)−C(5) and designated as a distinctive deoxyribose marker.[41] There is a coupletlike VCD feature at ∼981(−)/964(+) cm^{-1}, which is present persistently in the VCD spectra of other octamers.[27]

d(CCTGGTCC)·d(GGACCAGG)-*cis*-DDP (II). The spectra of the unplatinated (**I**) and platinated (**II**) duplexes (Figures 1 and 2, respectively, and Table 1) show pronounced differences in VCD and less so in absorption. Most prominently, the shoulder in absorption at 1618 cm^{-1} of **I** developed into an intense peak at 1623 cm^{-1} for **II**. The band centered at 1589 cm^{-1} of **I** has shifted to 1587 cm^{-1} with increased intensity. The intensity of the weak band at 1402 cm^{-1} of **I** has increased manifold upon platination. Changes in peak positions and relative intensities also occurred in the phosphate region. The strongest peak at 1085 cm^{-1} in **I** decreased in intensity, relative to the shoulder at 1075 cm^{-1}, and now reveals two distinct bands with apparent maxima at 1089 cm^{-1} and 1079 cm^{-1}. The former shoulder at 1062 cm^{-1} shifted to 1056 cm^{-1}, whereas the band at 1018 cm^{-1} remained almost the same, in regard to position and shape. The absorption at 971 cm^{-1} shifted to 969 cm^{-1} with an apparent shoulder to higher wavenumbers. Finally, the bands at ∼900 cm^{-1} of **I** obviously increased in intensity and the spectrum shows distinct absorption peaks at 914, 890, and 877 cm^{-1}.

The VCD spectrum of **II** changed even more extensively. The C(2)=O couplet of thymine of **I** is expected near 1718(+)/1707(−) cm^{-1}, but apparent noise in this region precludes a definitive determination. The couplet at 1700(+)/1689(−) cm^{-1} in **I** has shifted to 1697(+)/1687(−) cm^{-1}. The 1687(+)/1682(−) cm^{-1} couplet has moved to 1681(+)/1675(−) cm^{-1} without the clear shoulder in absorption of **I**. It is significant that the 1671(−)/1659(+) cm^{-1} couplet has changed sign to 1668(+)/1662(−) cm^{-1}, whereas the couplet at ∼1657(−)/1647(+) cm^{-1} has barely shifted to 1654(−)/1643(+) cm^{-1}, while that at 1642(+)/1633(−) has remained in essentially the same position. Neither of these modes shows any notable differences in absorption. The next VCD features of **II**, between ∼1635(−) and ∼1602(+) cm^{-1}, are totally absent in the spectrum of the unplatinated octamer. This segment in the spectrum indicates the principal structural distortion caused by the platinum lesion, as detected by VCD. The newly emerged couplets suggest significantly different stacking interactions, as a consequence of the distorted conformation upon platination. Specifically, new couplets appeared at 1631(+)/1619(−) cm^{-1}, which belongs to the new strong absorption at 1623 cm^{-1}, and 1610(−)/1602(+) cm^{-1}. The former can be assigned without hesitation to adenine. Both the VCD and absorption bands appeared persistently in d(A_4TATCATTGG)·d(CCAATGATAT$_4$),[35] the antiparallel hairpin d($T_8C_4A_8$),[35] the triple helices of poly(dA)·poly(dT) triple,[42] and poly(rA)·poly(rU) double and triple helices.[37] The new couplet at 1610(−)/1602(+) cm^{-1} is baffling. If there is a corresponding absorption, it must be hidden beneath the strong 1623 cm^{-1} band. In terms of its distinctive appearance and its resemblance to a similar feature in the platinated duplex of d(CCTCTGGTCTCC)·d(GGAGACCAGAGG),[32] it is clearly related to the formation of the platinum complex and may well arise from the C−N(D_2) stretch of guanine. The next group of couplets in **II**—at 1594(+)/1585(−) cm^{-1}, 1571(−)/1564(+) cm^{-1}, and 1550(+)/1542(−) cm^{-1}—almost exactly replicates

those of **I**. The first of these couplets displays its corresponding absorption at 1587 cm^{-1} with much increased intensity, compared to **I**. The absorption counterparts of the two VCD features that follow are not well-defined and are hidden under the broad band contours. The weak VCD couplet at 1538(+)/1530(−) cm^{-1} in **II**, with its corresponding absorption at 1532 cm^{-1}, was also found in **I**. The 1510(+)/1502(−) cm^{-1} couplet, not seen in **I**, corresponds to the absorption at 1506 cm^{-1} in **II**. The same VCD feature was noticed in $d(C)_8$[35] and was persistently present in octadeoxyribonucleotides.[27] There is another VCD couplet at 1496(+)/1488(−) cm^{-1} in **II** that is not visible in **I**; the origin of this couplet is not clear. The glycosidic bond shows a reasonably intense absorption at 1403 cm^{-1} in **II** and a possible hint of a weak VCD couplet at 1409(+)/1399(−) cm^{-1}. Similar, but less intense, features were noticed in **I**, with a possibly inverted VCD signal.

The main VCD couplet in the sugar−phosphate region at 1091(−)/1081(−) in **II** has experienced minor changes upon platination, implying that the backbone has not been affected much by the platinum lesion. There is a well-defined couplet in **II** at 1114(+)/1104(−) cm^{-1} that has no clear counterpart in absorption. Its analogue in **I**, occurring at 1109(+)/1101(−) cm^{-1}, was associated with PO_2^- and C−O sugar modes.[36,39] The 1079(−)/1071(+) couplet of **II** reproduces a similar feature in **I** almost identically. The distinct VCD couplet at 1054(+)/1047(−) cm^{-1} in **I** associated with the broad shoulder in absorption at ∼1050 cm^{-1} is visible in **II** as an appreciably large couplet at 1060(+)/1045(−) cm^{-1}. The corresponding absorption must be hidden beneath the broad shoulder marked as 1056 cm^{-1}.

Discussion

Structural Changes of d(CCTGGTCC)·d(GGACCAGG) and the Platinum Complex Determined by NMR. NMR measurements of the solution structure of the major product of cisplatin binding to the duplex indicated that the structure is kinked at the platination site.[43,44] Using molecular mechanics calculations and fitting the calculated NMR data, the kink was estimated to be in the range of 60°.[44] In the nuclear Overhauser effect (NOE) refined structure obtained by high-resolution NMR of the platinated adduct, the backbone conformation was found to be substantially different than the normal B-form, to accommodate the cisplatin lesion.[13] The bend toward the major groove was estimated to be 58°, which agrees with the molecular mechanics calculations, but appears to be larger than the 32°−40° bend derived from X-ray data[18] and gel electrophoresis of platinated DNA adducts.[45,46] Recent solution data suggested a 78° bend toward the major groove for the dodecameric analogue.[14] The significant bend opens and, at the same time, flattens the minor groove opposite to the Pt-coordination site. The deoxyribose conformation of the G4 nucleotide (Chart 1) is C3′-endo, whereas that of G5 is C2′-endo. C2′-endo sugar puckers were also predicted for the rest of the double helix. The dihedral angle between the guanine rings of G4 and G5 was determined to be 23°, consistent with the roll of 26° derived from X-ray results[18] but considerably less than the 49° value found in solution.[13] The refined structure also predicted minimal disruption of the base pairing[13] but did not support the possible hydrogen bonding between one of the amine ligands and a phosphate oxygen implied by X-ray.[17]

Effects of Platination on the Absorption and VCD Spectra. Comparison of the infrared absorption and VCD spectra of the unmodified duplex and its *cis*-DDP adduct reveals the conformational changes that take place upon binding. The main differences occur for the Pt-coordination site. The estimated 23° roll at the fourth base-pair step (G4pG5, Chart 1) distorts the entire double helical structure.[13] Platinum coordination also shifts the G4−C13 and G5−C12 base pairs out of order, thereby disrupting the stacking between T3−G4 and G5−T6. This interpretation is supported by the significant intensity decrease of all VCD couplets in the 1750−1500 cm^{-1} range upon platination. By the same reasoning, we would have expected that the 1718(+)/1707(−) cm^{-1} couplet should have disappeared as a result of the loss of stacking interaction, as indeed it did. We attribute the new couplet at 1631(+)/1619(−) cm^{-1} and the considerably increased intensity of the 1623 cm^{-1} absorption band to interaction between A11 and A14, which requires that the G4−C13 and G5−C12 base pairs are pulled out toward the major groove. The entire structure is kinked to such an extent that the two adenine bases come close enough together to interact with each other. The possibility of such an extreme conformation has not been articulated before.[13] A plausible explanation is that we observe the complex sufficiently early, before isomerization that leads to the *inter*strand adduct has taken place to an appreciable extent. As our VCD data suggest, the oligomer structure beyond the site of the platinum lesion and before isomerization is less distorted, which agrees with the NMR measurements. We expected the significant roll at G4pG5 to cause concomitant destacking between C13−C12, but this is not evident from the VCD spectra. The small downshift of the C═O couplet of cytosine to 1654(−)/1643(+) cm^{-1} most probably arises from an overall distortion of the duplex, whereas the interactions between C1−C2 and C7−C8 remain intact. Judging by the minor downshift of the couplet at 1700(+)/1689(−) cm^{-1} and the larger shift of the 1687(+)/1682(−) cm^{-1} couplet, the CT stacking between C2−G15 and T3−A14 and the corresponding CT stacking at the other end is affected by the platinum lesion but is still maintained. It is the fourth base step between G4pG5 connected to the Pt atom via the N7 atoms of the guanines where the most-extreme changes occurred in the VCD spectra. The couplet at 1671(−)/1659(+) cm^{-1} associated with GG stacking has reversed its sign and has narrowed to 1668(+)/1662(−) cm^{-1}. The inverted sign of the main VCD couplet, which is normally and typically observed for the Z-form, cannot be interpreted as an opposite helical twist of the base pairs. The solution[13,14] and crystal studies[17,18] of the same octameric and similar dodecameric oligonucleotides indicate a right-handed structure. Moreover, an inverted helical twist would also have reversed the sign of the phosphate signals,[29,47] which is not evident in the VCD spectrum of **II**. This sign inversion, which is observed mainly for the carbonyl stretch of adjacent guanines, can be explained by a local reorientation of the oscillating carbonyl dipoles of G4pG5, resulting in sign inversion of their in-phase and out-of-phase combinations. The signs of other VCD couplets (with the possible exception for C═N stretching of cytosine) remain the same and only their wavenumbers have shifted, according to the shift of the corresponding absorption bands.

The main VCD features in the phosphate region closely resemble those of the unmodified duplex. The negative lobe of the couplet arising from the symmetric PO_2^- vibration at 1089(−)/1082(+) cm^{-1} has experienced a negligible shift to 1091(−)/1081(+) cm^{-1}. The second component of the main couplet at 1079(−)/1072(+) cm^{-1} in **I**, attributed to coupled vibrations of the phosphodiester backbone and sugar modes, also remains unchanged. There is some change in the markers of the C2′-endo sugar puckers.[41] The 1054(+)/1047(−) cm^{-1} couplet in **I** is no longer a clear feature in **II**. The apparently

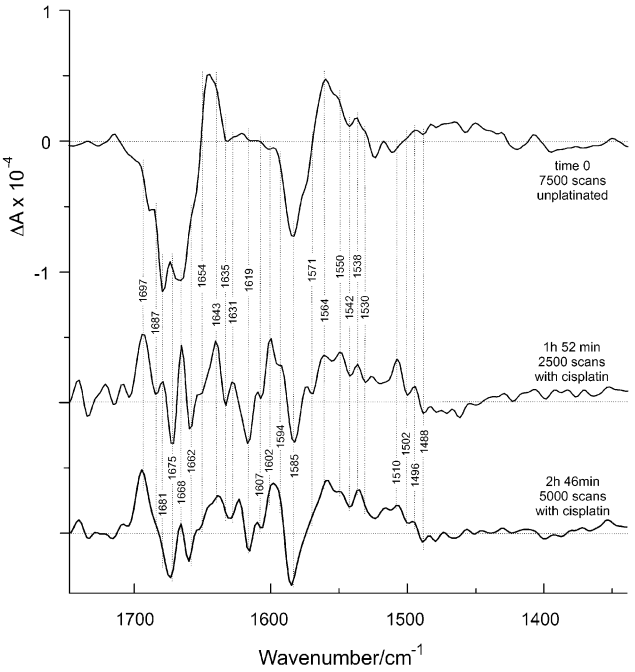

Figure 3. VCD spectra of the d(CCTGGTCC)·d(GGACCAGG)−cisplatin complex, as a function of time in the 1700−1400 cm^{-1} region.

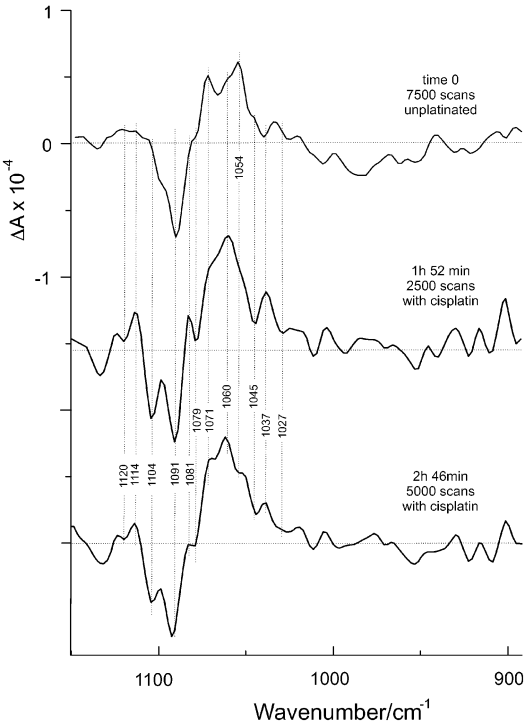

Figure 4. VCD spectra of the d(CCTGGTCC)·d(GGACCAGG)−cisplatin complex as a function of time in the 1150−950 cm^{-1} region.

separate couplets of **I** merged in the platinated duplex, giving a coupletlike feature at 1060(+)/1045(−) cm^{-1}, which most likely consist of overlapping bands. The different absorptions below 1000 cm^{-1} in **II**, which are due to sugar modes, suggest by their different intensities that some changes have taken place in the sugar conformations upon platination.

Isomerization from Intrastrand Crosslinks to Interstrand Crosslinks. The VCD spectrum of the platinated duplex (Figure 2) was recorded ∼2 h after both strands were annealed. Slow isomerization from *intra*strand to *inter*strand crosslinks was observed over a period of several weeks;[13] therefore, we reduced the number of scans to 2500 for the ac data (∼1 h) and 50 dc scans (∼2 min) before and after the complete ac collection, expecting to capture the spectra of the platinated complex before much of the conversion takes place. Although we followed the isomerization for 17 h, we report here only the first three hours. The spectra obtained in the ranges of 1700−1500 and 1150−900 cm^{-1}, taken over the shorter period, likely represent average snapshots of the course of isomerization (Figures 3 and 4, respectively, for VCD; absorption spectra are not shown). The VCD spectra are changing slowly with time; therefore, it is difficult to determine whether the first two VCD spectra of the complex are accurate representations of the *intra*strand crosslinks or include the beginning of isomerization. The maximal distortion observed upon platination brings A11 and A14 sufficiently close to enable stacking interactions (Chart 1); thus, we believe that the VCD spectra in Figures 3 and 4 are mainly those of the platinated G4pG5 complex. The absorption spectra of the complex do not change to any noticeable extent, whereas VCD yielded remarkably different spectra every hour for as long as we monitored the isomerization process.

NMR, electrospray mass spectrometry, and high-pressure liquid chromatography (HPLC) profile analysis performed on this sequence indicate unambiguously that d(CCTGGTCC)·d(GGACCAGG) isomerizes into an *inter*strand *cis*-DDP crosslinked octamer duplex with crosslinks between G4 and G9.[13] We find clues in the VCD spectra taken after ∼3 h that confirm this conclusion. Although it seems feasible to extract more-detailed information about the conversion from the spectra to date, more controlled experiments will be necessary to identify the intermediate structures in more-reliable detail. It is nonetheless possible to point out a few details. For example, the couplets of the G4pG5 complex at 1668(+)/1662(−) cm^{-1} and 1641(+)/1635(−) cm^{-1} (C6═O of G and C4═O of T, respectively) diminish in intensity (Figure 3, middle spectrum versus the bottom spectrum). Substantial transformations also occur for the VCD couplets located in the 1660−1585 cm^{-1} region, whereas the couplet at ∼1598(−)/1585(+) cm^{-1} in the free duplex remains unchanged as time progressed. The structural changes resulting from the isomerization also affect the octamer backbone (Figure 4). The transition from (G4pG5)−*cis*-$[Pt(NH_3)_2]^{2+}$ *intra*strand coordination to a more-stable G4 to G9 *inter*strand crosslinks should also impact the VCD signals in the phosphate region. For example, while the main VCD couplet 1089(−)/1082(+) cm^{-1} is preserved, the couplets corresponding to the various sugar modes undergo noticeable changes.

Conclusions

On the basis of our previous experiences, we wanted to extend our understanding of structural changes of DNA when coordinated with metal ions by applying vibrational circular dichroism (VCD) to *cis*-diamminedichloroplatinum(II) (*cis*-DDP)−oligonucleotide adducts. More importantly, for further investigations of cisplatin complexes by VCD, it will be essential to correlate VCD features with structures determined by other means, specifically NMR[13,14] and X-ray crystallography,[17,18] thereby establishing whether VCD is capable of providing information complementary to NMR and X-ray methods and revealing new and/or different structural aspects.

The principal objectives for investigating the cisplatin complex with the octamer duplex d(CCTGGTCC)·d(GGACCAGG) by infrared absorption and VCD spectroscopy were twofold. First, we wanted to expand our ability to interpret the effects of changes to DNA structure that are due to metal-

ion coordination on VCD spectra generally and comparatively. Second, we wanted to know explicitly whether VCD is capable of distinguishing between the parent and the platinated duplex, and to what extent VCD may be able to contribute new or different information if characteristic changes should appear in the spectra. We can respond affirmatively to both these questions. Although the absorption spectra between the octamer and its platinated complex differ somewhat, the VCD spectra display those differences in much greater and more intricate detail. This is true for both regions accessible at this time of development, namely, the carbonyl and in-plane ring vibrations of the bases and the phosphodiester−deoxyribose backbone. Guided by the previous NMR and X-ray crystallographic investigations,[13,18] we were able to deduce meaningful interpretations of the VCD spectra of the duplex and its platinum adducts. Although the interpretations cannot yield structural information in as much numerical detail as either NMR or X-ray crystallography, the qualitative results are no doubt distinctive and complement the other two techniques. In that sense, VCD is likely to be useful for systems for which neither NMR nor X-ray methods can be applied in practice. One particularly telling example is the evolution with time of the isomerization of the G4pG5 cisplatin adduct. The VCD spectra display the process very clearly. Optimization of the potentially available information will require more targeted and carefully controlled experiments, which will not pose undue difficulties. In terms of the difficulties of assigning the observed features in the VCD spectra, we note that model calculations using modern ab initio techniques are within reach, as we demonstrated recently.[36] Finally, if lingering doubt remains regarding an uncertainty about recognizing even small VCD features as being real, the reproducibility of the spectra even with time provide a degree of confidence in the assignments.

Acknowledgment. We thank the Core DNA Services of the University of Calgary for synthesizing the oligonucleotide and the Department of Chemistry at the University of Calgary for providing the necessary infrastructure for the research to be take place. Funding from the Natural Sciences and Engineering Research Council of Canada (NSERCC) (to J.H.v.d.S. and H.W.) and from the Alberta Heritage Foundation for Medical Research (through an AHFMR Scholar award to D.T.) is gratefully acknowledged.

References and Notes

(1) Cohen, S.; Lippard, S. J. *Prog. Nucleic Acid Res. Mol. Biol*. **2001**, *67*, 93−130.
(2) Jamieson, E.; Lippard, S. J. *Chem. Rev*. **1999**, *99*, 2467−2498.
(3) Gelasco, A.; Lippard, S. J. In *Metallopharmaceuticals I*: *DNA Interactions, Topics in Biological Inorganic Chemistry*; Clarke, M. J., Sadler, P., Eds.; Springer-Verlag: Heidelberg, Germany, 1999; pp 1−43.
(4) Reedijk, J. *Pure Appl. Chem.* **1987**, *59*, 181−192.
(5) Reedijk, J. *Chem. Commun.* **1996**, 801−806.
(6) Fichtinger-Schepman, A. M. J.; van der Veer, J. L.; den Hartog, J. H. J.; Lohman, P. H. M.; Reedijk, J. *Biochemistry* **1985**, *24*, 707−713.
(7) Reeder, F.; Guo, Z.; Murdoch, P. D.; Corazza, A.; Hambley, T. W.; Berners-Price, S. J.; Chottard, J. C.; Sadler, P. J. *Eur. J. Biochem.* **1997**, *249*, 370−382.
(8) Sullivan, S. T.; Ciccarese, A.; Fanizzi, F. P.; Marzilli, L. G. *J. Am. Chem. Soc.* **2001**, *123*, 9345−9355.
(9) Reed, E.; Ozols, R. A.; Tarone, R.; Yuspa, S. H.; Poirier, M. C. *Proc. Natl. Acad. Sci. U.S.A.* **1987**, *84*, 5024−5028.
(10) Teuben, J. M.; Bauer, C.; Wang, A. H.-J.; Reedijk, J. *Biochemistry* **1999**, *38*, 12305−12312.
(11) Blommaert, F. A.; van Dijk-Knijnenburg, H. C. M.; Dijt, F. J.; den Engelse, L.; Baan, R. A.; Berends, F.; Fichtinger-Schepman, A. M. J. *Biochemistry* **1995**, *34*, 8474−8480.
(12) Fichtinger-Schepman, A. M. J.; van Dijk-Knijnenburg, H. C. M.; van der Velde-Visser, S. D.; Berends, F.; Baan, R. *Carcinogenesis* **1995**, *16* (6), 2447−2453.
(13) Yang, D.; van Boom, S. S. G. E.; Reedijk, J.; van Boom, J. H.; Wang, A. H.-J. *Biochemistry* **1995**, *34*, 12912−12921.
(14) Gelasco, A.; Lippard, S. J. *Biochemistry* **1998**, *37*, 9230−9239.
(15) Chaconas, G.; van de Sande, J. H. *Methods Enzymol.*, **1980**, *65*, 75−85.
(16) den Hartog, J. H. J.; Altona, C.; van der Elst, H.; van der Marel, G. A.; Reedijk, J. *Inorg. Chem.* **1985**, *24*, 983−986.
(17) Takahara, P. M.; Rosenzweig, A. C.; Frederick, C. A.; Lippard, S. J. *Nature* **1995**, *377*, 649−652.
(18) Takahara, P. M.; Frederick, C. A.; Lippard, S. J. *J. Am. Chem. Soc.* **1996**, *118*, 12309−12321.
(19) Tinoco, I., Jr. *Radiat. Res.* **1963**, *20*, 133−139.
(20) Deutsche, C. W.; Moscowitz, A. *J. Chem. Phys.* **1968**, *49*, 3257−3272.
(21) Snir, J.; Frankel, R. A.; Schellman, J. A. *Biopolymers* **1975**, *14*, 173−196.
(22) Gulotta, M.; Goss, D. J.; Diem, M. *Biopolymers* **1989**, *28*, 2047−2058.
(23) Keiderling, T. A. In *Circular Dichroism and Conformational Analysis of Biomolecules*; Fasman, G. D., Ed.; Plenum: New York, 1996; pp 555−598.
(24) Diem, M. *Spectroscopy* **1995**, *10*, 38−43.
(25) Maharaj, V.; Tsankov, D.; van de Sande, J. H.; Wieser, H. *J. Mol. Struct.* **1995**, *349*, 25−28.
(26) Maharaj, V.; Rauk, A.; van de Sande, J. H.; Wieser, H. *J. Mol. Struct.* **1997**, *408*/*409*, 315−318.
(27) Maharaj, V. Ph.D. Thesis, The University of Calgary, Calgary, AB, Canada, 1996.
(28) Andrushchenko, V.; van de Sande, J. H.; Wieser, H. *Vibr. Spectrosc*. **1999**, *19*, 341−345.
(29) Andrushchenko, V.; van de Sande, J. H.; Wieser, H.; Kornilova, S.; Blagoi, Yu. *J. Biomol. Struct. Dyn.* **1999**, *17*, 545−560.
(30) Andrushchenko, V. Ph.D. Thesis, The University of Calgary, Calgary, AB, Canada, 2000.
(31) Andrushchenko, V.; Leonenko, Z.; Cramb, D.; van de Sande, H.; Wieser, H. *Biopolymers* **2002**, *61*, 243−260.
(32) Tsankov, D.; Kalisch, B.; van de Sande, J. H.; Wieser, H. *Biospectroscopy*, in press.
(33) Andrushchenko, V.; van de Sande, J. H.; Wieser, H. *Biopolymers*, in press, 2003.
(34) Tsankov, D.; Eggimann, T.; Wieser, H. *Appl. Spectrosc.* **1995**, *49*, 132−138.
(35) Krasteva, M. Ph.D. Thesis, The University of Calgary, Calgary, AB, Canada, 2002.
(36) Andrushchenko, V.; Wieser, H.; Bour, P. *J. Phys. Chem. B* **2002**, *106*, 12623−12634.
(37) Andrushchenko, V.; Blagoi, Yu.; van de Sande, J. H.; Wieser, H. *J. Biomol. Struct. Dyn*. **2002**, *19*, 889−906.
(38) Wang, L.; Keiderling, T. A. *Biochemistry* **1992**, *31*, 10265−10271.
(39) Tsuboi, M. *Appl. Spectrosc. Rev.* **1969**, *3*, 45−90.
(40) Letellier, R.; Ghomi, M.; Taillandier, E. *J. Biomol. Struct. Dyn.* **1989**, *4*, 755−768.
(41) Dohy, D.; Ghomi, M.; Taillandier, E. *J. Biomol. Struct. Dyn.* **1989**, *6*, 741−754.
(42) Wang, L.; Pancoska, P.; Keiderling, T. *Biochemistry* **1994**, *33*, 8428−8435.
(43) den Hartog, J. H. J.; Altona, C.; van Boom, J. H.; van der Marel, J. H.; Haasnoot, C. A. G.; Reedijk, J. *J. Biomol. Struct. Dyn.* **1985**, *2*, 1137−1154.
(44) Herman, F.; Kozelka, J.; Stoven, V.; Guittet, E.; Girault, J.-P.; Huynh-Dinh, T.; Igolen, J.; Lallemand, J.-Y.; Chottard, J.-C. *Eur. J. Biochem*. **1990**, *194*, 119−133.
(45) Rice, J. A.; Crothers, D. M.; Pinto, A. L.; Lippard, S. J. *Proc. Natl. Acad. Sci. U.S.A.* **1988**, *85*, 4158−4161.
(46) Bellon, S. F.; Lippard, S. J. *Biophys. Chem*. **1990**, *35*, 179−188.
(47) Wang, L.; Keiderling, T. A. *Biophys. J.* **1994**, *67*, 2460−2467.